

Inverse Scattering of a Lossy Dielectric Object by the Genetic Algorithm

Yi-Da Wu

Electrical Engineering Department,
Tamkang University
Tamsui, Taiwan, R.O.C.
e-mail: g8350106@tkgis.tku.edu.tw

Chien-Ching Chiu

Electrical Engineering Department,
Tamkang University
Tamsui, Taiwan, R.O.C.
e-mail: chiu@ee.tku.edu.tw

Abstract: In this paper, an efficient optimization algorithm for solving the inverse problem of a two-dimensional homogeneous lossy dielectric object is investigated. A homogeneous lossy dielectric cylinder of unknown permittivity scatters the incident wave in free space and the scattered fields are recorded. Based on the boundary condition and the incident field, a set of nonlinear surface integral equation is derived. The imaging problem is reformulated into optimization problem and the genetic algorithm is employed to reconstruct the shape and the dielectric constant of the object. Numerical results show that the permittivity of the cylinders can be successfully reconstructed even when the permittivity is fairly large. The effect of random noise on imaging reconstruction is also investigated.

Keyword: Inverse scattering, Genetic algorithm, Lossy dielectric object

I. Introduction

In this paper, the inverse problem of the lossy dielectric cylinder with unknown cross-section and dielectric constant is investigated. The inverse scattering problem of lossy dielectric objects has been a subject of considerable importance in noninvasive measurement, medical imaging, and biological application. In the past 20 years, many rigorous methods have been developed to solve the exact equation. However, inverse problem of this type are difficult to solve because of its ill-posedness and nonlinearity. As a result, many inverse problems are reformulated as optimization problems. General speaking, two main kinds of approaches have been developed. The first is based on the gradient search approach such as the Newton-Kantorovitch method [1],[2], the Leveberg-Marguart algorithm [3],[4] and the successive-overrelaxation method [5]. This method is highly dependent on the initial guess and tends to get

trapped in a local extreme. In contrast, the second approach is based on the genetic algorithm [6],[7]. It usually converges to the global extreme of the problem, no matter what the initial estimate is [8].

By using the equivalent surface current technique [9], the inverse problem is efficiently solved in this study. Instead of dividing the cross-section of the tested object into many cells, the object surface is dividing into small segments such that the equivalent surface electric and magnetic current distributions can be obtained numerically by solving the one-dimensional integral equation.

By applying the genetic algorithm and the moment method, the inverse problem can be solved as optimization problem. We need only define the range of the parameter corresponding to the shape function and the permittivity of the cylinder. Good reconstruction is obtained as multi-incident waves are applied to get the measured data. In Section II, the theoretical formulation is presented. In Section III, numerical results for lossy objects are given. Finally, some conclusions are drawn in Section IV.

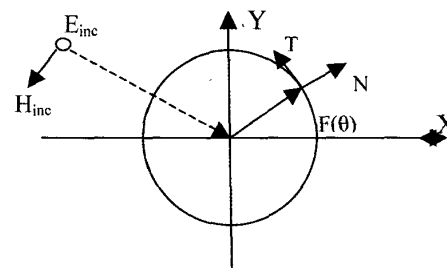


Fig. 1 Geometry of problem in (x,y) plane.

II. Theoretical Formulation

Consider a homogeneous lossy dielectric cylinder located in free space as shown in Fig.1. The cross section of the object is of starlike shape, such that it can be described in polar coordinates by $\rho = F(\theta)$. The permittivity and permeability of free space and the lossy dielectric object are denoted by (ϵ_0, μ_0) and (ϵ_2, μ_2) , respectively. In our case, ϵ_2 is complex number.

The dielectric object is illuminated by an incident plane wave whose electric field vector is parallel to the z axis (i.e., TM polarization). We assume that time dependence of the field is harmonic with the factor $e^{j\omega t}$. Then, the incident electric and magnetic fields can be given by

$$\vec{E}^{inc}(x, y) = E_0 e^{-jk_0(x \sin \phi - y \cos \phi)} \hat{z}$$

$$k_0^2 = \omega^2 \epsilon_0 \mu_0$$

$$\vec{H}^{inc}(x, y) = -E_0 \sqrt{\frac{\epsilon_0}{\mu_0}} (\cos \phi \hat{x} + \sin \phi \hat{y}) e^{-jk_0(x \sin \phi - y \cos \phi)}$$

where ϕ is the incident angle and k_0 is the free-space wave number.

Since the tangential components of \vec{E} and \vec{H} fields should be continuous across the surface of the dielectric object, we can derive two integral equations as follows.

$$\hat{n} \times \vec{E}^{inc}(F(\theta), \theta) = -\hat{n} \times \int_0^{2\pi} [j\omega(\mu_2 G_2(k_2 r_0) + \mu_0 G_0(k_0 r_0))] \vec{J}(\theta') + \vec{M}(\theta') \times \nabla'(G_2(k_2 r_0) + G_0(k_0 r_0)) d\theta' \quad (1)$$

$$\hat{n} \times \vec{H}^{inc}(F(\theta), \theta) = -\hat{n} \times \int_0^{2\pi} [j\omega(\epsilon_2 G_2 + \epsilon_0 G_0)] \vec{M}(\theta') - \vec{J}(\theta') \times \nabla'(G_2(k_2 r_0) + G_0(k_0 r_0)) - \rho_m(\theta') \nabla' \left(\frac{G_2(k_2 r_0)}{\mu_2} + \frac{G_0(k_0 r_0)}{\mu_0} \right) d\theta' \quad (2)$$

with

$$G_2(k_2 r_0) = \frac{j}{4} H_0^{(2)}(k_2 r_0) \quad G_0(k_0 r_0) = \frac{j}{4} H_0^{(2)}(k_0 r_0)$$

$$k_i = \omega \sqrt{\mu_i \epsilon_i}, \quad i = 0, 2$$

$$r_0(\theta, \theta') = |\vec{r} - \vec{r}'|$$

$$= \sqrt{F^2(\theta) + F^2(\theta') - 2F(\theta)F(\theta') \cos(\theta - \theta')}$$

$$\vec{J}(\theta) = \sqrt{F^2(\theta) + F'^2(\theta)} \vec{J}_s(\theta)$$

$$\vec{M}(\theta) = \sqrt{F^2(\theta) + F'^2(\theta)} \vec{M}_s(\theta)$$

$$\rho_m(\theta) = \sqrt{F^2(\theta) + F'^2(\theta)} \rho_{ms}(\theta), \quad \rho_{ms} = \frac{j}{\omega} \nabla \cdot \vec{M}_s$$

where $\vec{J}_s(\theta)$ and $\vec{M}_s(\theta)$ are the equivalent surface electric and magnetic current densities, \hat{n} is the outward unit normal on the object surface, and $G_0(k_0 r_0)$, $G_2(k_2 r_0)$ are the Green's functions in free-space and in a homogeneous space with relative dielectric constant $\epsilon_r = \epsilon_2 / \epsilon_0$ respectively. Here $H_0^{(2)}$ stands for the Hankel function of the second kind of zeroth order.

For TM case, the electric field has only one component along the z axis such that the scattered electric field \vec{E}^s at the point (x, y) outside the scatterer can be expressed by

$$\vec{E}^s(x, y) = \int_0^{2\pi} [j\omega \mu_0 G_0(k_0 \xi) \vec{J}(\theta') + \vec{M}(\theta') \times \nabla' G_0(k_0 \xi)] d\theta' \quad (3)$$

with

$$\xi = \sqrt{(x - F(\theta') \cos \theta')^2 + (y - F(\theta') \sin \theta')^2}$$

In order to solve the direct problem for a given $F(\theta)$ and ϵ_2 (let $\mu_2 = \mu_0$), the moment method is applied. By using pulse basis functions $\{P_n(\theta)\}$ for expanding the unknown functions $\vec{J}(\theta)$ and $\vec{M}(\theta)$ into N_d terms, we have

$$\vec{J}(\theta) = J(\theta) \hat{z} \cong \sum_{n=1}^{N_d} \alpha_n P_n(\theta) \hat{z}$$

$$\vec{M}(\theta) = M(\theta) \hat{i}(F(\theta), \theta) \cong \sum_{n=1}^{N_d} \beta_n P_n(\theta) \hat{i}(F(\theta), \theta)$$

$$P_n(\theta) = \begin{cases} 1, & \text{on } \Delta \ell_n \\ 0, & \text{otherwise} \end{cases}$$

($\Delta \ell_n$ means the arc length of the object surface from

$$\theta = \frac{2\pi(n-1)}{N_d} \text{ to } \theta = \frac{2n\pi}{N_d})$$

By employing the point-matching technique, the above integral equations (1) and (2) can be transformed into matrix form as

$$\begin{cases} [E^{inc}]_{n \times 1} = [C_1]_{n \times n} [J]_{n \times 1} + [C_2]_{n \times n} [M]_{n \times 1} \\ [H^{inc}]_{n \times 1} = [C_3]_{n \times n} [J]_{n \times 1} + [C_4]_{n \times n} [M]_{n \times 1} \end{cases} \quad (4)$$

and the scattered electric field \bar{E}^s in Eqn.(3) can be transformed as

$$\begin{aligned} \bar{E}^s(x, y) = & -\sum_{n=1}^N \left\{ \int_{\Delta \ell} \frac{-\omega \mu_0 H_0^{(2)}(k_0 \xi)}{4} \alpha_n \right. \\ & \left. + j \frac{k_0 H_1^{(2)}(k_0 \xi)}{\sqrt{F^2(\theta') + F'^2(\theta')} \xi} \beta_n d\theta' \right\} \hat{z} \quad (5) \end{aligned}$$

For the direct scattering problem, the scattered field \bar{E}^s is calculated by assuming that the shape functions are known. This can be achieved by first solving $\bar{J}(\theta)$ and $\bar{M}(\theta)$ using (1) and (2) and then the scattered field outside the scatterer can be calculated from Eqn. (5). It serves as the measured data of the inverse problem for the purpose of numerical simulation.

For the inverse problem, we assume the approximate center of the scatter, which in fact can be any point inside the scatterer, is known. Then the shape $F(\theta)$ function can be expanded as:

$$F(\theta) = \sum_{n=0}^N B_n \cos(n\theta) + \sum_{n=1}^N C_n \sin(n\theta)$$

where B_n and C_n are real number to be determined, and $2N+1$ is the number of unknown coefficients for shape function. In the inversion procedure, the steady-state genetic algorithm is used to minimize the following cost function:

$$CF = \left\{ \frac{1}{M_t} \sum_{m=1}^{M_t} |E^{s,exp}(\bar{r}_m) - E^{s,cal}(\bar{r}_m)|^2 |E^{s,exp}(\bar{r}_m)|^2 \right\}^{1/2}$$

where M_t is the total number of the measurement. $E^{s,exp}(\bar{r})$ and $E^{s,cal}(\bar{r})$ are the measured scattered field and the calculated scattered field respectively.

The parameters B_n and C_n are coded using Gray code, and the processes of reproduction, mutation and crossover are employed to optimize B_n and C_n . Here, we use the steady-state genetic algorithm for our image problem. The variance of steady-state genetic algorithm is to insert a temporary population which composes of the parent populations and the new individuals generated by crossover and mutation. Offspring individuals are then reproduced using rank selection scheme until the original population size is reached again. Steady-state genetic algorithm has not only the characteristic of faster convergence [10][11], but also the lower rate of crossover. As a result, it is a suitable scheme to effectively save the calculation time for the inverse problem as compared with the generational G.A..

III. Numerical Results

In this section, we report some numerical results of using the scheme described in Section II. Lossy homogeneous dielectric objects are taken into account. The sensitivity of this method to random noise in the scattered field is also investigated.

Let us consider a dielectric cylinder located in the free space. The permittivity of the dielectric object ϵ_2 is assumed in the following examples. The frequency of the incident wave is chosen to be 3 GHz and the corresponding free-space wavelength is $\lambda = 0.1m$. To reconstruct the shape and the permittivity, the dielectric objects in the following examples are illuminated by plane waves of unit amplitude from three directions ($\phi = 0^\circ, 120^\circ, 240^\circ$), and the measurement points ($M_t = 16$) are equally separated on a circle of radius $r_m = 0.5m$. The size of the object considered in each example is on the order of half wavelength. Note that the simulated result using only one incident wave is much worse than that using two incident waves. However, in order to get accurate results, three incident waves are used here. Numerically, for direct and inverse problems, $N_d = 100$ is set for the direct problem and $N_d = 50$ for the inverse problem. The number of unknowns, including the shape function coefficients ($2N+1$) and the relative permittivity ϵ_r and the loss term, is $2N+3$, in total.

The first example, the shape function (object A) is

chosen to be $F(\theta) = 0.04 + 0.01 \sin(4\theta)$ m, and the relative permittivity of the object is $\epsilon_r = 2.56 - j * 1.12$. The reconstructed shape function of the best population member is plotted in Fig.2 (a). The r.m.s. error (DF) of the reconstructed shape $F^{cal}(\theta)$ and the relative error (DIPE) of ϵ_r^{cal} (include real part and image part) with respect to the exact values versus generation are shown in Fig. 2(b). The r.m.s. error DF is about 1.2%, $DIPE_{real} = 3.8\%$, and $DIPE_{image} = 4.2\%$ in final.

In Fig.3 object B with the shape $F(\theta) = 0.04 + 0.015 \sin(3\theta)$ m is considered and the dielectric constant of the object is $\epsilon_r = 5 - j * 1.2$. The result that $DF = 6.2\%$, $DIPE_{real} = 1.1\%$, and $DIPE_{image} = 3.5\%$ in final. The Fig. 4 shows the reconstructed results under the condition that the measured scattered field is contaminated by noise $c + jd$, where c and d are independent random variables with uniform distribution. The values of c and d are distributed from $-\alpha_n$ to α_n , where α_n is defined as the r.m.s value of the scattered field times the relative noise level. The relative noise levels include 0.04, 0.08, 0.1, 0.2, and 0.3 for simulation purpose. In here, it can be seen that good reconstruction is obtained when the relative noise level is below 0.1.

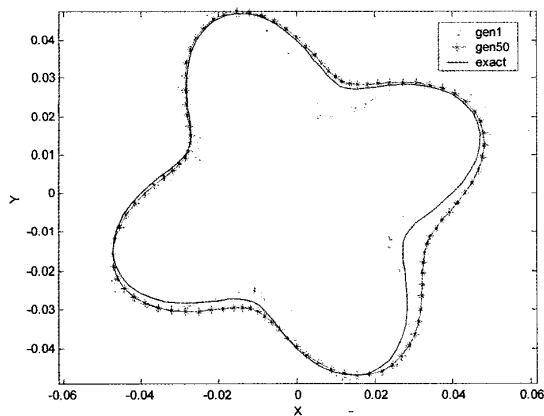


Fig. 2 Reconstructed results for shape A.

(a) Shape function for first example. The solid curve represents the exact shape, while the star curves are calculated shape in iteration process.

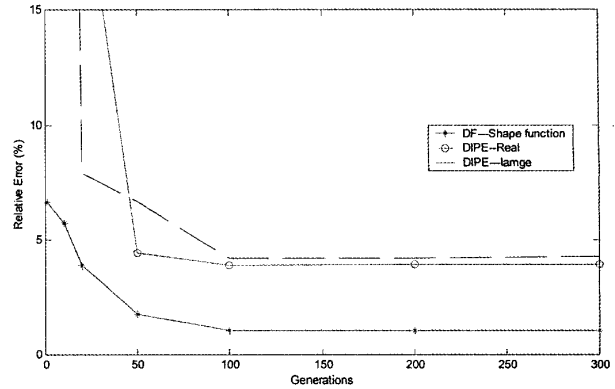


Fig. 2 Reconstructed results for shape A.

(b) Shape-function error and permittivity error in each generation.

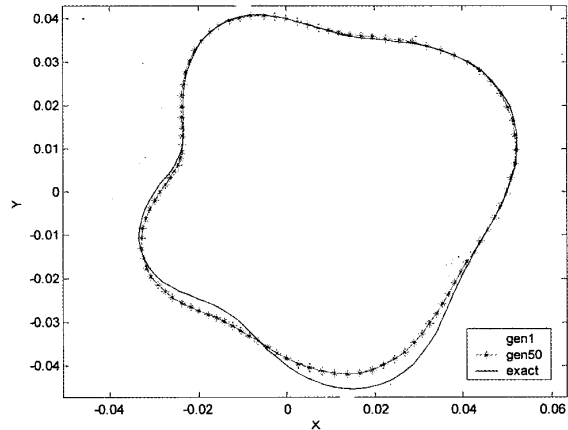


Fig. 3 Reconstructed results for shape B.

(a) Shape function for second example. The solid curve represents the exact shape, while the star curves are calculated shape in iteration process.

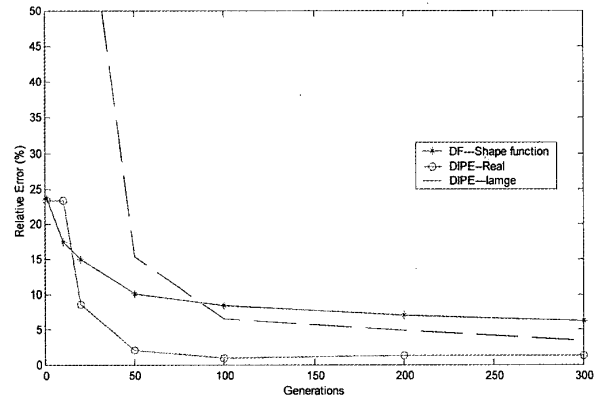


Fig. 3 Reconstructed results for shape B.

(b) Shape-function error and permittivity error in each generation.

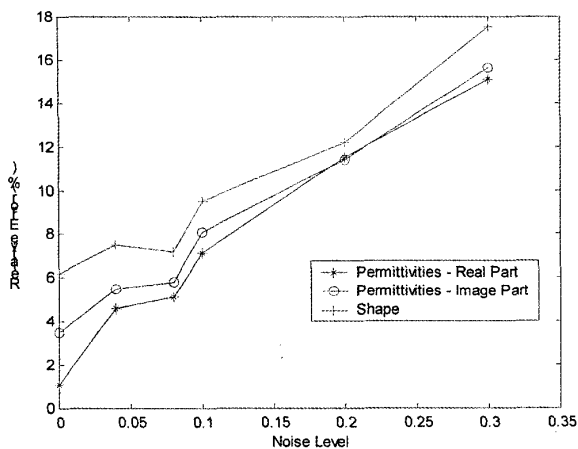


Fig. 4 Shape error and the relative permittivity errors as functions of noise level.

IV. Conclusions

We have presented a study of applying the genetic algorithm to reconstruct the shapes and relative permittivity of a homogeneous lossy dielectric cylinder. Based on the equivalence principle, boundary condition and measured scattered fields, we have derived a set of nonlinear surface integral equations and reformulated the imaging problem into an optimization problem. By using the genetic algorithm, the shape and dielectric constant of the object can be successfully reconstructed even when the dielectric constant is fairly large. Numerical results are presented and good reconstruction is obtained.

References

- [1] A. Roger, "Newton-Kantorovitch algorithm applied to an electromagnetic inverse problem," *IEEE Trans. Antennas Propagat.*, vol. 29, 232-238, 1981.
- [2] C. C. Chiu and Y. W. Kiang, "Electromagnetic imaging for an imperfectly conducting cylinders," *IEEE Trans. Microwave Theory Tech.*, vol. 39, pp. 1632-1639, Sept. 1991.
- [3] D. Colton and P. Monk, "A novel method for solving the inverse scattering problem for time-harmonic acoustic waves in the resonance region II," *SIAM J. Appl. Math.*, vol. 46, pp. 506-523, June 1986.
- [4] F. Hettlich, "Two methods for solving an inverse conductive scattering problem," *Inverse Problems*, vol. 10, pp. 375-385, 1994.
- [5] R. E. Kleinman and P. M. van den Berg, "Two-dimensional location and shape reconstruction," *Radio Sci.* vol. 29, pp. 1157-1169, July-Aug. 1994.
- [6] C. C. Chiu and P. T. Liu, "Image reconstruction of a perfectly conducting cylinder by the genetic algorithm," *IEE Proc.-Micro. Antennas Propagat.*, vol. 143, pp.249-253, June 1996.
- [7] C. C. Chiu and W. T. Chen, "Electromagnetic imaging for an imperfectly conducting cylinder by the genetic algorithm," *IEEE Trans. Microwave Theory and Tec.*, vol. 48, pp. 1901 -1905, Nov. 2000.
- [8] D. E. Goldgerg, "*Genetic Algorithm in Search, Optimization and Machine Learning*," Addison-Wesley, 1989.
- [9] H. T. Lin and Y. W. Kiang, "Microwave imaging for a dielectric cylinder," *IEEE Trans. Microwave Theory Tech.*, vol.42, pp.1572-1579, 1994.
- [10] F. Vavak and T. C. Fogarty, "Comparison of steady state and generational genetic algorithms for use in nonstationary environments," *Proceedings of IEEE International Conference on Evolutionary Computation*, pp. 192-195, 1996.
- [11] J. Michael Johnson and Yahya Rahmat-Samii, "Genetic algorithms in engineering electromagnetics," *IEEE Trans. Antennas Propagat.*, vol.39, pp. 7-21, Aug. 1997